

# EFFECT OF GRAPHITE MICROPARTICLE SIZE ON THE GAS PERMEABILITY AND FRIABILITY OF REFRACTORY FOUNDRY COATINGS

G. MILANOVA<sup>a</sup>, K. PETROV<sup>a</sup>, M. ZAGORSKI<sup>a</sup>, R. RANGELOV<sup>a</sup>, M. KANDEVA<sup>a,b\*</sup>

<sup>a</sup> *Technical University of Sofia, <sup>a</sup> Faculty of Industrial Technology,*

<sup>b</sup> *Tribology Center, 8 Kl. Ohridsky Blvd., 1797 Sofia, Bulgaria*

*Email: kandevam@gmail.com*

## ABSTRACT:

The present paper concerns casting properties (gas permeability and friability) of samples applied with refractory coatings with dimensions of the refractory filler - 60  $\mu\text{m}$ , 80  $\mu\text{m}$ , 100  $\mu\text{m}$  and 120  $\mu\text{m}$  respectively. The investigated coatings are designed to prevent the formation of sintering effect during the production of iron alloy castings (steel and cast iron). The base on which those paints are applied represents standard test samples for determining the casting properties of moulding and core mixtures made of croninng sand. The obtained results show that the increase of the size of the graphite particles leads to an increase in gas permeability and almost does not affect friability.

*Keywords:* casting, refractory coatings, gas permeability, friability.

## INTRODUCTION

Casting in sand moulds often causes the formation of sintering defect on the surface of the castings. Slag is a layer of moulding materials tightly adhering to the surface of the casting, which is formed when the metal interacts with the mould. Its thickness can reach 30 - 40 mm. Depending on the nature of the bond between the grains of the adhering mixture, it is accepted to define scorch as mechanical, chemical and thermal<sup>1</sup>.

Mechanical sintering is that in which the connection between the individual grains of the moulding or core mixture is effected by the metal that has penetrated into the pores of the mould.

Thermal sintering is characterized by the fact that in it the sand grains are joined into a monolithic mass without the direct involvement of the melt. In this case, the connection is created

from easily melting compounds formed at high temperatures as a result of the reactions that occur between the components of the moulding compound. Sands that contain easily fusible impurities have a marked tendency to form sintering. The thermal burn is not firmly connected to the casting and separates from it without much effort. Most often, it forms the outer layer of the crust from mechanical or chemical sintering<sup>2</sup>.

The separation of mechanical sintering from chemical sintering is conditional. At the metal-form (mould) interface, chemical reactions always take place, which facilitate the penetration of the liquid metal into the pores of the casting mould.

Sintering is one of the most common defects in ferrous metal castings. According to statistics, an average of 12 - 15% of the time required for the production of castings is spent on its cleaning<sup>3</sup>.

In order to obtain a burn, it is necessary that the liquid metal or the products of its interaction with the moulding mixture penetrate into the pores of the casting mould to a depth greater than the radius of the sand grains. At a lower penetration depth, the layer of moulding compound is easily separated from the surface of the casting, on which imprints of the sand grains remain. They make the surface of the casting rough, but roughness according to BDS is not classified as a defect. In some countries, the roughness of the walls of the castings is evaluated according to special standards. The larger grain size of the moulding sand, the rougher the casting<sup>4</sup>. The metal penetrates the pores of the casting mould while it is in a liquid state, i.e. during the period from its filling to the formation of the surface skin of the casting<sup>5</sup>.

Mechanical sintering is very difficult to separate from castings and its cleaning requires considerable effort and resources. This is due to the great strength of the metal penetrated between the sand grains. The strength of the mechanical burn can reach  $20\text{--}22 \cdot 10^5 \text{ N/m}^2$ . According to modern scientific theories, liquid penetration of metal into the pores of the casting mould occurs under the action of capillary forces and metallostatic pressure. The magnitude and direction of action of the capillary forces are determined by the surface tension of the melt at the metal-form interface and the associated wetting of the grains of the liquid metal mixture. The metallostatic pressure is determined by the product of the height of the melt above the penetration zone and the specific gravity of the metal<sup>6</sup>. The other factors that determine the depth of penetration are the viscosity of the melt, the size of the pores between the sand grains, the gas pressure in those pores, and the time the metal remains in the liquid state. Taking into account Poiseuille's law, the depth of penetration of the metal in the form  $l, m$ , can be approximately determined by the formula:

$$l = r \sqrt{\frac{\tau}{\eta} \left( H\gamma + \frac{2\sigma}{r} \cos \alpha - p_{gas} \right)}$$

where:

$\sigma$  is the surface tension of the melt at the metal-form interface, N/m;

$\alpha$  - the wetting angle of the sand grains from the metal;

$\eta$  - the viscosity of the liquid metal, Pa.s (N.s/ m<sup>2</sup>);

$r$  - the average size of the pores between the grains, m;

$\tau$  - the time during which the metal remains in a liquid state in the pores of the form, s;

$p_{gas}$  - the pressure of the gases in the pores of the mould, Pa (N/m<sup>2</sup>);

$H$  - the height of the liquid metal ladder, m;

$\gamma$  - the specific weight of the metal, N/m<sup>3</sup>.

Each of these factors is greatly influenced by the processes involved in obtaining the liquid metal, making and pouring the mould<sup>6</sup>.

Surface tension arises from the unbalanced forces that act on the surface of the liquid metal (fig. 1).

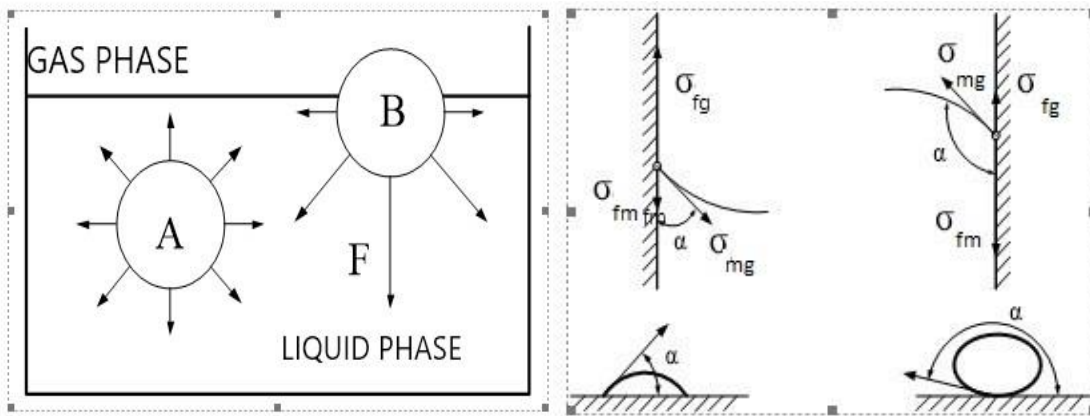


**Fig. 1** Forces creating surface tension

**Fig. 2** Surface tensions

On each particle A which is inside the liquid forces that balance each other act. However, the forces acting on particle B are not balanced because its upper surface is subjected to the action of the gas phase, the concentration of which is very small. Therefore, the particles of the outer layer act on the resultant forces F, directed perpendicular to the surface of the liquid. These forces create the surface tension. Under its action, small amounts of liquid spilled on a horizontal surface take the form of drops, as if wrapped in a thin, strong and elastic skin<sup>7</sup>. During its movement, the

metal melt simultaneously establishes contact with the walls of the mould and with the gas phase. At the contact point of the three phases (Fig. 2) the surface tensions  $\sigma$  form-gas ( $\sigma_{fg}$ ),  $\sigma$  form-metal ( $\sigma_{fm}$ ) and  $\sigma$  metal-gas ( $\sigma_{mg}$ ) act. When  $\sigma_{fg} > \sigma_{fm}$ , the angle  $\alpha$  between  $\sigma_{fm}$  and  $\sigma_{mg}$  is sharp. Then the meniscus of the liquid in capillary sections, such as the channels between grains of sand, is concave and it will rise without the need for this hydrostatic pressure. If  $\sigma_{fg} < \sigma_{fm}$ , the angle  $\alpha$  is greater than  $90^\circ$ . Then the meniscus of the liquid is convex, it does not wet the form and will not climb into capillary sections. In order to penetrate them, a hydrostatic pressure is needed, the value of which must be greater than the resistance that the capillaries offer to the movement of the liquid<sup>8</sup>.

One of the main methods for preventing the formation of sintering is the use of refractory coatings. The aim of the research is to obtain a highly effective refractory coating on a graphite basis for casting iron alloys in strong moulds<sup>11</sup>. To achieve this goal, it is necessary to make standard test samples of croning sand and prepare four coats of different sizes of refractory filler<sup>9</sup>.

## EXPERIMENTAL

Standard samples are made of quartz sand 01PK016 coated with novolac resin (fig. 3).



**Fig. 3** Test samples

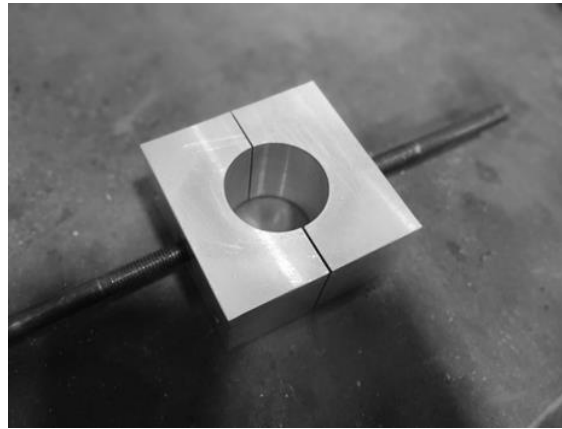


**Fig. 4.** Test tools

For a standard cylindrical sample with dimensions diameter  $d = 50 \pm 0.2$  mm, height  $h = 50 \pm 1$  mm, a tool is designed and manufactured (fig. 4)

The following materials are used to make the casting coating:

Graphite -50%: Graphite has the role of a refractory filler, which is used in the production of cast iron, carbon steel and non-ferrous alloys. Graphite is not suitable in the production of low carbon and manganese steel castings because of chemical incompatibility between it and the liquid

metal<sup>10-11</sup>. Due to its wide application, graphite and respectively graphite coating are most often chosen as a type of coating by foundries in Bulgaria and Europe.

Methyl alcohol -50%: The reason for investigating alcohol-based rather than water-based coatings is their wide application and economy compared to water-based coatings, which require mandatory subsequent drying in special dryers.

Novolac resin is used as a binder - 5% of the total amount of graphite and methyl alcohol.

The components are mixed in a special "basket" type mill, which, in addition to homogenizing the ingredients, also grinds the graphite particles.

Several types of coatings are sampled and are processed in the mill for different periods of time as follows:

- GCA120 - without grinding - particle size 120 µm;
- GCA100 - 15 minutes grinding - particle size 100 µm;
- GCA80 - 30 minutes grinding - particle size 80 µm;
- GCA60 - 45 minutes grinding - particle size 60 µm.

After preparing the coatings with different particle sizes, they are applied to the sand mould. The density of the coating after grinding for all types is 1.5 g/s m<sup>3</sup>. Samples of each type of coating are taken and further diluted to a 10 second batch viscosity.

The coatings are applied by dipping the samples, after which they are ignited to burn off the solvent.

Gas permeability is called the property of moulding and core mixtures to pass gases<sup>2</sup>. It is one of the most important properties of mixtures, determining the possibility of filling the working cavity of the mould with liquid metal and avoiding gas defects in castings<sup>8</sup>. It depends on the size and uniformity of the grains of the moulding sands, on the amount of binder and water, on the degree of compaction of the mould, etc. It is measured by the amount of gases that have passed through a body of a certain area and thickness at a unit of pressure in a unit of time

$$K = \frac{Q \cdot h}{F \cdot p \cdot \tau}$$

where:

Q is the amount of air passed through the sample, in cm<sup>3</sup>;

h - the height of the sample in cm;

$F$  - the cross-sectional face of the sample in  $\text{cm}^2$ ;

$p$  - the air pressure in the sample in  $\text{N}/\text{cm}^2$ ;

$T$  - the time for passage of air with volume  $Q$  through the sample in min.

To determine the gas permeability, a device is used, creating air pressure  $p = 100$  mm water column and measuring the pressure before the sample. The air of the instrument is passed into the sample through calibrated inlets, and when examining mixtures with low gas permeability - up to 50 units, an opening with a diameter of  $\varnothing = 0.5$  mm is used, and for mixtures with a gas permeability of more than 50 units - an opening with a diameter of  $\varnothing = 1.5$  mm. The pressure gauge of the instrument (position 3 on fig. 5) has three scales - one for tare of the instrument and two others corresponding to the two calibrated holes for reading the gas permeability of the test body<sup>12-13</sup>. It should be noted that the results obtained do not correspond to the actual gas permeability of the casting moulds. The data is used only for comparative characteristics of the mixtures.

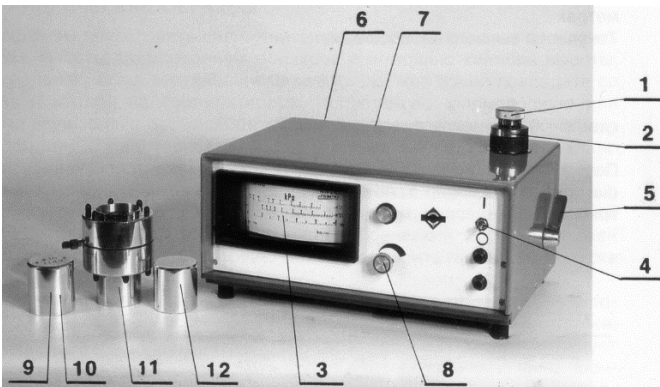


**Fig. 5** Device for determining gas permeability

- 1-handle for switching the different calibrated holes
- 2-tip with a rubber sleeve for sealing the sleeve with the test body
- 3-manometer scale with readings for gas permeability and air pressure
- 4-switch for turning on the electrical supply
- 5-lever for sealing the sleeve with the test body
- 6-pressure gauge locking lever during transport
- 7-adjusting screw for resetting the pressure gauge
- 8-screw for adjusting the pressure of the blown air
- 9-control sleeve with hole  $\varnothing 0.5$  mm
- 10-control sleeve with hole  $\varnothing 1.5$  mm
- 11-sleeve for dried samples
- 12-cap

The surface strength of the mould and core is of great importance to the quality of the casting<sup>1</sup>. The surface strength is characterized by friability - the percentage loss of the mass of the samples after appropriate processing<sup>14-15</sup>. The standard sample body coated with the investigated coating is weighed on a balance (fig. 6) with an accuracy of 0.1 g and placed on the rollers of the instrument (fig. 7). The sample is rolled for 15 min, then weighed again. Friability is indicated by the difference in sample weights expressed as a percentage.

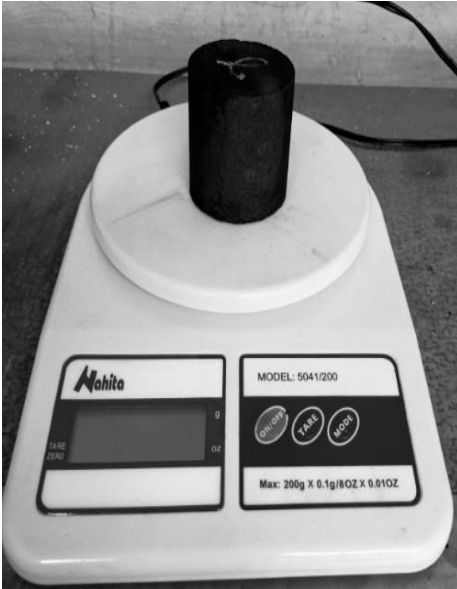


**Fig. 6** Scale



**Fig. 7** Apparatus for determining friability

## RESULTS AND DISCUSSION

The gas permeability and friability results of the three trials and their arithmetic mean for each coating are presented in Tables 1 and 2.

**Table 1.** Gas permeability

no	sample	1	2	3	Average value
1	GCA120	80	86	93	<b>85.3</b>
2	GCA100	65	63	71	<b>66.3</b>
3	GCA80	55	58	62	<b>58.3</b>
4	GCA60	50	48	54	<b>50.7</b>
5	NGCA	220	230	217	<b>215.7</b>

**Table 2.** Friability

n	samples	1			2			3			Average value
		before	after	difference	before	after	difference	before	after	difference	
1	GCA120	145.7	145.3	0.4	150.6	150.2	0.4	149.3	148.9	0.4	<b>0.4</b>
2	GCA100	144.3	144.0	0.3	149.5	149.1	0.4	150.6	150.3	0.3	<b>0.33</b>
3	GCA80	143.2	142.9	0.3	148.8	148.5	0.3	145.9	145.5	0.4	<b>0.33</b>
4	GCA60	145.1	145.0	0.1	149	148.8	0.2	147.9	147.7	0.2	<b>0.17</b>

Fig. 8 shows the microhardness diagram of coatings with different graphite particle sizes and fig. 9 – a graphical view of the dependence of microhardness on particle size.

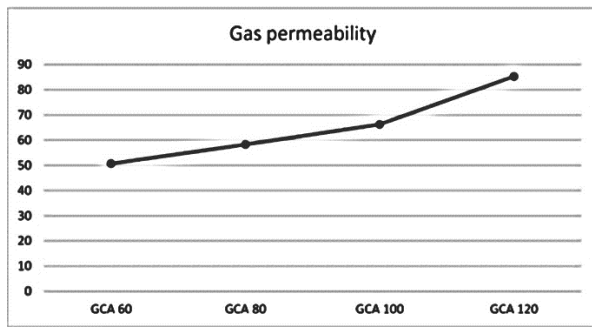


**Fig. 8.** Gas permeability diagram of coatings with different graphite particle sizes

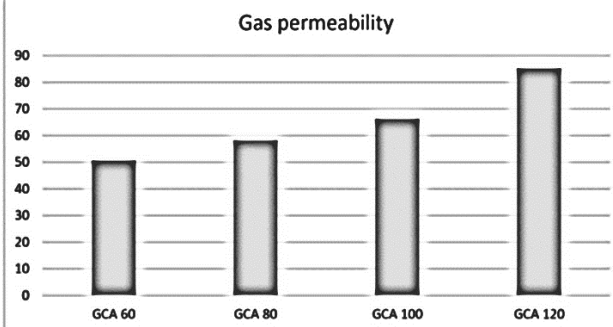


**Fig. 9.** Graphical dependence of gas permeability on graphite particle size

The graphs on the figures show that as the size of the graphite particles increases, the gas permeability of the coating increases. This can be explained by the fact that with larger refractory fillers, the pores between them are larger and this facilitates the passage of gases. Fig. 10 shows the friability diagram of coatings with different sizes of graphite particles, and fig. 11 – their graphic dependence. The results from the study of friability show that the size of the graphite particles does not affect the friability of the coating. The slight difference in the obtained values could be explained by the larger mass of the larger particles.

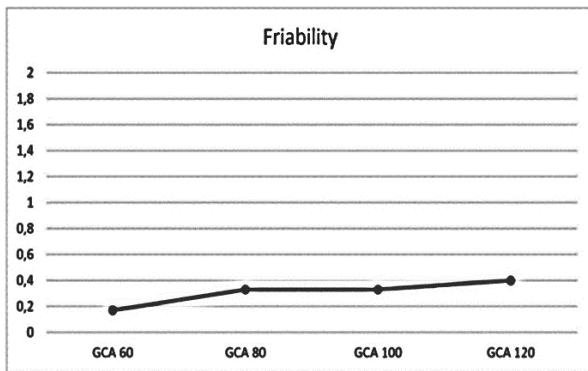


**Fig. 10** Diagram of friability of coatings with different sizes of graphite particles

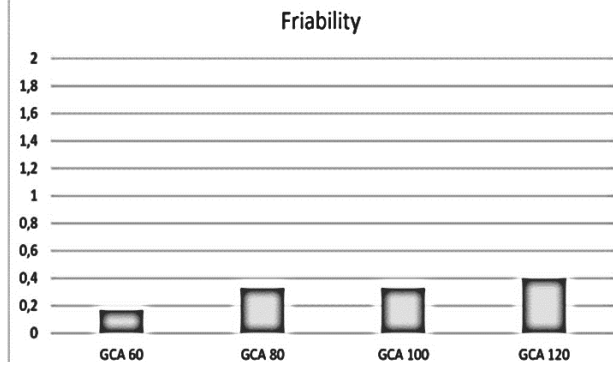


**Fig. 11.** Graphical dependence of friability on graphite particle size



## CONCLUSIONS

Four types of anti-stick coatings with sizes of graphite particles respectively - 60  $\mu\text{m}$ , 80  $\mu\text{m}$ , 100  $\mu\text{m}$  and 120  $\mu\text{m}$  are investigated at the same viscosity of the suspension. The different particle sizes are obtained by grinding, and the coating is applied by dipping standard coated sand samples in a slurry of the tested coatings. Results for the gas permeability and friability of the coatings are obtained. The effect of refractory filler size on gas permeability is found to be proportional- larger particles provided, better gas permeability even with small difference than the smaller particles. It is also found that the size of the graphite particles does not affect the friability.

## ACKNOWLEDGMENT

The current research is funded by The Research and Development Sector (R&DS) of the Technical University-Sofia within a research project in aid of a doctoral student with contract No 222ПД0005-05.

## REFERENCES

1. G. ANGELOV, Technology of foundry production, S., Technika (1988).
2. Manual for laboratory exercises on technology, machines and equipment in foundry production, Sofia, ed. of TU – Sofia (2010).
3. R. TODOROV, P. PESHEV, Defects in ferrous metal castings, S. Technika (1980).
4. T. A. BURNS, “The Foseco Foundryman's Handbook,” Pergamon Press, Staffordshire (1986).
5. I. D. KASCHEEV, N. Y. NOVOZHILOV, E. V. TSAREVSKII, V. A. PEREPELITSYN, V. A. RYABIN and N. F. SELIVERSTOV, “Re-fractory Coatings for Foundry Moulds and Cores,” Journal of Refractories and Ceramics, Vol. 23, pp. 36-139 (1982).
6. AFS, “Moulding Methods and Materials,” 1st Edition, The American Foundrymen's Society, Illinois (1962).
7. S. D. CHASTAIN, “A Sand Casting Manual for the Small Foundry,” Jacksonville Publishers, Florida, Vol. 1 (2004).

8. L. HORVATH, "Coatings Go Beyond Appearance to Provide Quality Control,<http://www.Foundrymag.com/Classes/Article/articledraw.aspx>. (2010).
9. F. W. PURSALL, "Coatings for Moulds and Cores," K. Straus, Ed., Applied Science in the Casting of Metals, Pergamon Press, Oxford (1970).
10. R. E. MOORE, "Refractories, Structure and Properties," Encyclopedia of Materials: Science and Technology, pp. 8079-8099 (2001).
11. N. SCHUTZE, Control Limits for the Drying of Water Based Coatings, Foseco, Foundry Practice. 255, June (2011).
12. L.JAAMROZOWICZ, J. ZYCH & T. SNOBKIEWICZ. The Research of Desiccation Rates Selected Protective Coating Used on Mould and Sand Cores. Archive of Foundry Engineering. 13(01), 45-50 (2013).
13. J. JAKUBSKI, S. DOBOSZ, & P. JELINEK, The influence of the protective coating type on thermal deformation of casting cores. Archives of Foundry. 5(15) (2005).
14. B. SARUM, Ductile and Compacted Graphite Iron Casting Skin -Evaluation, Effect on Fatigue Strength and Elimination, B. Ohio State University, Page 103-106 (2013).
15. G.L. DI MUOIO, N. SKAT TIEDJE, B. BUDOLPH JOHANSEN, Critical control variables for the coating of furan bonded sand with water based foundry coating. World foundry congress, 19-21 May 2014. Bilbao, Spain (2014).